

# We are IntechOpen, the world's leading publisher of Open Access books Built by scientists, for scientists

4,800

Open access books available

122,000

International authors and editors

135M

Downloads

Our authors are among the

154

Countries delivered to

TOP 1%

most cited scientists

12.2%

Contributors from top 500 universities



WEB OF SCIENCE™

Selection of our books indexed in the Book Citation Index  
in Web of Science™ Core Collection (BKCI)

Interested in publishing with us?  
Contact [book.department@intechopen.com](mailto:book.department@intechopen.com)

Numbers displayed above are based on latest data collected.  
For more information visit [www.intechopen.com](http://www.intechopen.com)



# Data Association Techniques for Non-Gaussian Measurements

Stephen C. Stubberud<sup>1</sup> and Kathleen A. Kramer<sup>2</sup>

<sup>1</sup>*Oakridge Technology*

<sup>2</sup>*University of San Diego  
USA*

## 1. Introduction

In target tracking, the primary algorithm for estimating the target state has been the Kalman filter (Blackman, 1986) and (Blackman and Popoli, 1999). This workhorse algorithm and its nonlinear implementation, the extended Kalman filter (EKF), provide both an estimate of the target kinematic state, e.g. position and velocity, and an estimate of the error covariance associated with the target state (Brown, 1983). The linear Kalman filter is given as

$$\mathbf{K}_k = \mathbf{P}_{k|k-1} \mathbf{H}^T (\mathbf{H} \mathbf{P}_{k|k-1} \mathbf{H}^T + \mathbf{R}_k)^{-1} \quad (1a)$$

$$\mathbf{x}_{k|k} = \mathbf{x}_{k|k-1} + \mathbf{K}_k (\mathbf{z}_k - \mathbf{H} \mathbf{x}_{k|k-1}) \quad (1b)$$

$$\mathbf{P}_{k|k} = (\mathbf{I} - \mathbf{K} \mathbf{H}) \mathbf{P}_{k|k-1} \quad (1c)$$

$$\mathbf{x}_{k+1|k} = \mathbf{F} \mathbf{x}_{k|k} \quad (1d)$$

$$\mathbf{P}_{k+1|k} = \mathbf{F} \mathbf{P}_{k|k} \mathbf{F}^T + \mathbf{Q}_k \quad (1e)$$

where  $\mathbf{x}$  is the track estimate,  $\mathbf{H}$  is the output-coupling matrix that maps the track space to the measurement space,  $\mathbf{F}$  is the state-coupling matrix that models the target motion,  $\mathbf{z}$  is the measurement from the sensor,  $\mathbf{P}$  is the error covariance,  $\mathbf{K}$  is the Kalman gain that weights the residual or innovation,  $\mathbf{R}$  is the measurement error covariance, and  $\mathbf{Q}$  is the process noise. The subscript  $k$  is the scan,  $k|k$  indicates the update from the new measurement, and  $k+1|k$  denotes prediction. The basic premise of the Kalman filter is that the measurements are Gaussian random variables and the target motion's error or process noise is also Gaussian. For this reason, the Mahalanobis distance (Blackman, 1986) and (Mahalanobis, 1936)

$$(\mathbf{h}(\mathbf{x}_1) - \mathbf{z}_2)^T (\mathbf{H} \mathbf{P}_1 \mathbf{H}^T + \mathbf{R}_2)^{-1} (\mathbf{h}(\mathbf{x}_1) - \mathbf{z}_2) \quad (2)$$

has been used as a measure to determine how “close” a measurement is to a given track. The inner product measure of Eq. (2) weights the residual in measurement space by the error covariance:

$$\mathbf{HP}_1\mathbf{H}^T + \mathbf{R}_2 \quad (3)$$

Thus, a large covariance error reduced the effect of large differences. This chi-squared random variable has provided the primary scoring algorithm for the data association step in the tracking problem as seen in the Bowman model (Steinberg, Bowman, and White, 1999) in Fig. 1.

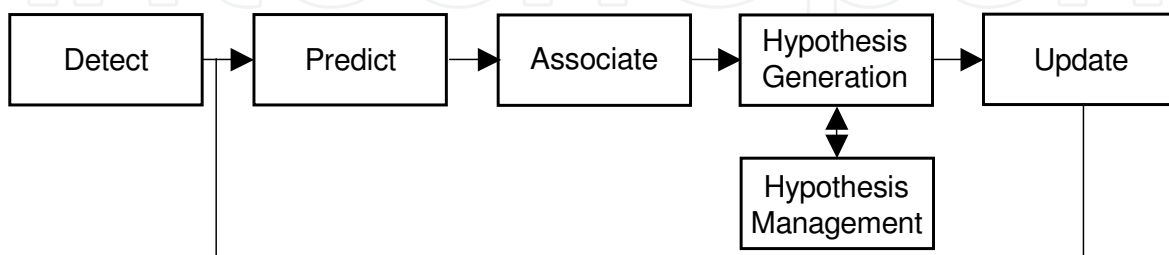


Fig. 1. Target Tracking Functional Flow.

While the Kalman filter has its strengths, the Gaussian assumption is not always accurate. As seen in Figure 2, a simplified model of a passive acoustic measurement is not well approximated by a Gaussian model. Near-field measurements of such a sensor have greater errors as shown in Figure 3. With terrain and mapping information, target limitations and sensor blockage (Figure 4) cannot be mapped without changing the underlying Gaussian assumption of the Kalman filter as done in (Yang and Blasch, 2009).

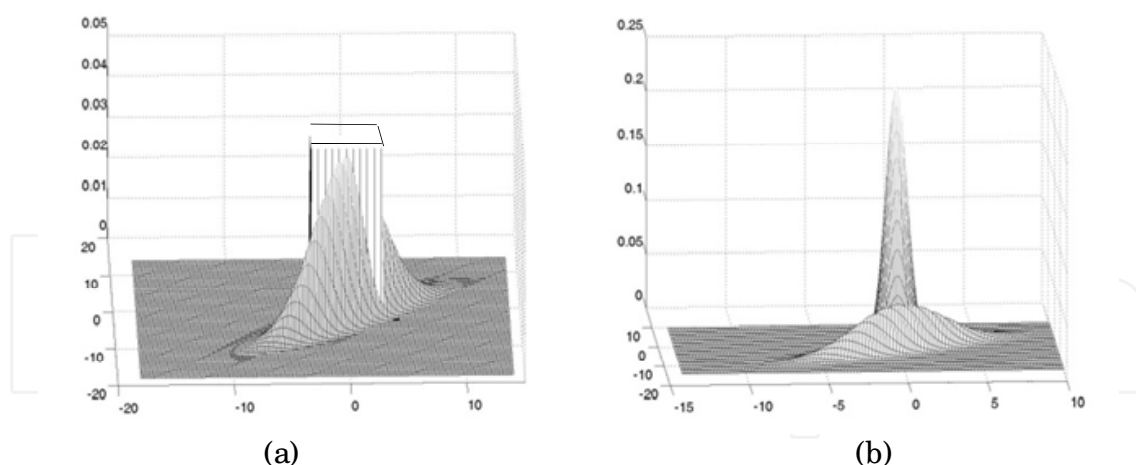


Fig. 2. a) Measurement Distributions – One with Uniform Distribution and One with Gaussian b) Measurement Distributions – With Gaussian Distribution Used to Approximate a Uniform Distribution

A number of techniques have been derived to handle these issues. Some of the basic techniques include the use of Gaussian sums (Alspach, 1970) and (Alspach and Sorenson, 1972) to approximate the non-Gaussian sensor measurements. The so-called unscented Kalman filter (UKF) (Haykin, 2002) and the particle filter (Arulampalam et al, 2002) use samples of the probability density functions to combine the random variables of the track

and measurement. In (Stubberud, 2003) and (Stubberud, 2000), a sequential estimator that can incorporate constraints on the target state without a Gaussian assumption was developed. The single Mahalanobis distance of Eq. (2) is not valid for the Gaussian sum and completely invalid for the other techniques.

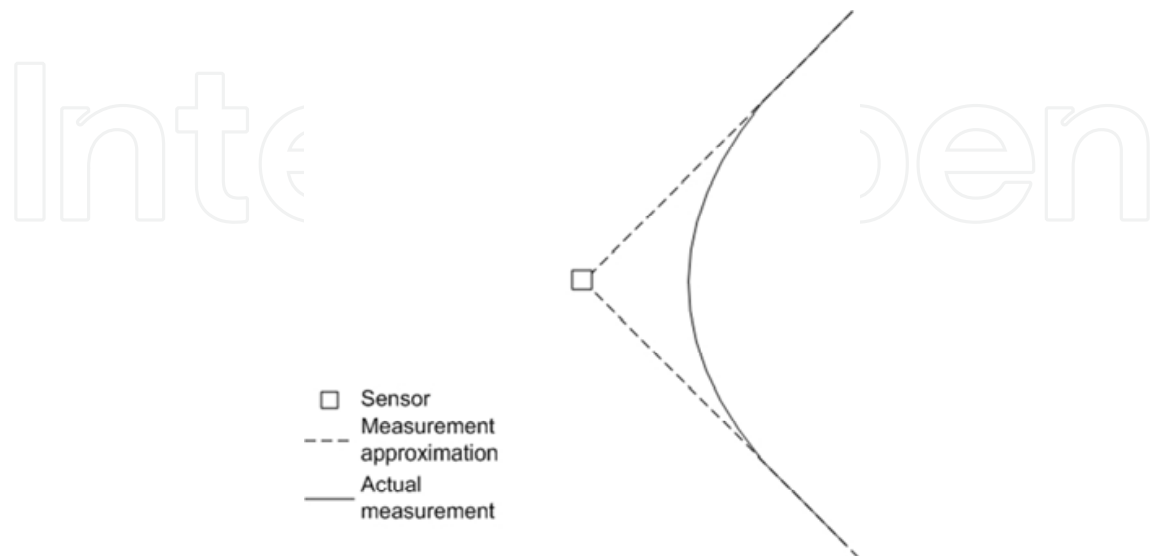


Fig. 3. Near field measurement error

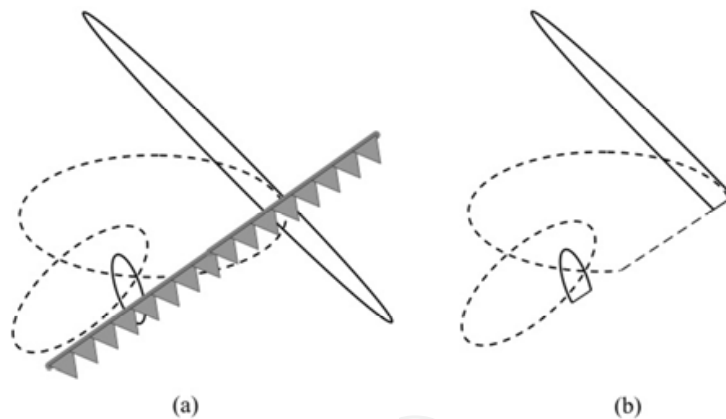


Fig. 4. Uncertainty error ellipses are affected by sensor blockage. a) Gaussian ellipses and blockage indicated; b) resulting alteration of ellipse.

Also, target tracking has grown beyond simple kinematic tracking. The use of classification information has also been incorporated into target track states. Usually, a Bayesian taxonomy (Pearl, 1988) or a Dempster-Shafer algorithm (Dempster, 1967) and (Shafer, 1976) has been employed to provide the scoring for the classification association of the measurement to the target state. The kinematic score is then combined with the classification score using a technique defined by the implementer.

Besides the improvement in the tracking algorithms, data fusion has grown well beyond the target tracking application. As defined in (Steinberg, Bowman, and White, 1999), fusion now covers a number of interpretations of information from a wide variety of sources. Applications are more varied than the military surveillance and targeting that founded the research. However, as discussed in (Stubberud, Shea, and Klammer, 2003) and (Llinas et al,

2004), the association step is still important. Techniques that do not rely on a Gaussian random variable are necessary.

In this chapter, an association technique that maps data into image representation is presented. The images are compared using a phase-only filter (POF) technique to provide a correlation score. The data can be from any source. Each source may contain an uncertainty measure or not. A single association score results.

The development of this effort begins with a previously developed fuzzy logic kinematic association scoring technique that did not rely on the Gaussian assumption. This approach provides the foundation for incorporation of uncertainty into the image representation. The fuzzy approach discussion is followed by the original image correlation technique without uncertainty. The uncertainty incorporation is then developed and example of tracking with kinematics and classification is provided

## 2. Data association using fuzzy logic

With the desire for more accurate target tracking (Smith and Singh, 2006) and the incorporation of terrain information into tracking systems (Shea et al, 2000) the use of Gaussian models for target tracks and their associated uncertainties became less desirable. While new methods for incorporating non-Gaussian measurements into track states were being developed, different metrics and association routines were being developed for measurements and tracks that were modeled as generic probability density functions. One such method used in some tracking system is the Dempster-Shafer method. This technique does not require any specific probability density function. It is a powerful tool but complex to implement. Other approaches that have been researched use fuzzy logic.

One fuzzy logic approach for association was developed to emulate the chi-squared metric (Stubberud and Lugo, 1999). The fuzzy logic approach used a linguistic model of two interpretations of the chi-squared metric for Gaussian tracks and measurements. Using this basic concept of fuzzy logic (Kosko, 1992), two interpretations of the chi-squared metric were used. The first, a mathematical description, was that the distance between the means was relative based on the size of the covariances. A layered fuzzy logic approach (see Figure 5) was developed where the size of the error covariances of the target and the measurement were used to generate the parameters of the membership functions of the antecedent with regards to the size of the residual.

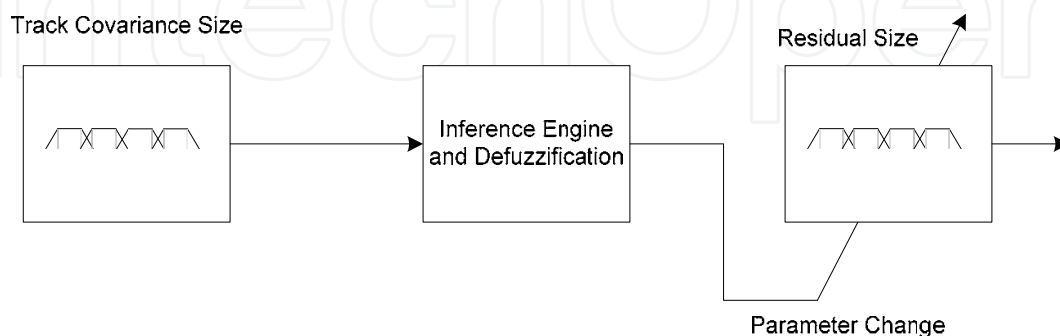


Fig. 5. Layered fuzzy logic is used to reduce computational explosions by making the parameters of membership functions dependent on inputs as opposed to adding to the inference engine.

The second interpretation, a graphical interpretation, determined amount of overlap that the 2-sigma ellipses for the measurements created relative to the maximum amount of overlap possible. Then the three inputs, residual size and the two percentages of overlap, are operated on by the inference engine, as shown in Figure 6, and that results in the association score. This approach was shown to have comparable behavior to the chi-squared metric in two standard challenge problems, crossing targets and closely spaced parallel targets.

The development of the fuzzy association scheme was then extended to handle the two cases where measurements and/ or tracks that had uniform probability density functions, (Stubberud and Kramer, 2006) and (Stubberud and Kramer, 2007). The first case considered two uniformly distributed representation. The association is performed using the graphical interpretation of overlapping areas. As seen in Figure 7, when the uniform distributions are being associated, the scoring can be looked at as the graphical interpretation. A percentage of overlap between the two density functions can be interpreted to give a score between 0 and 1. The fuzzy system operates on the overlapping region.

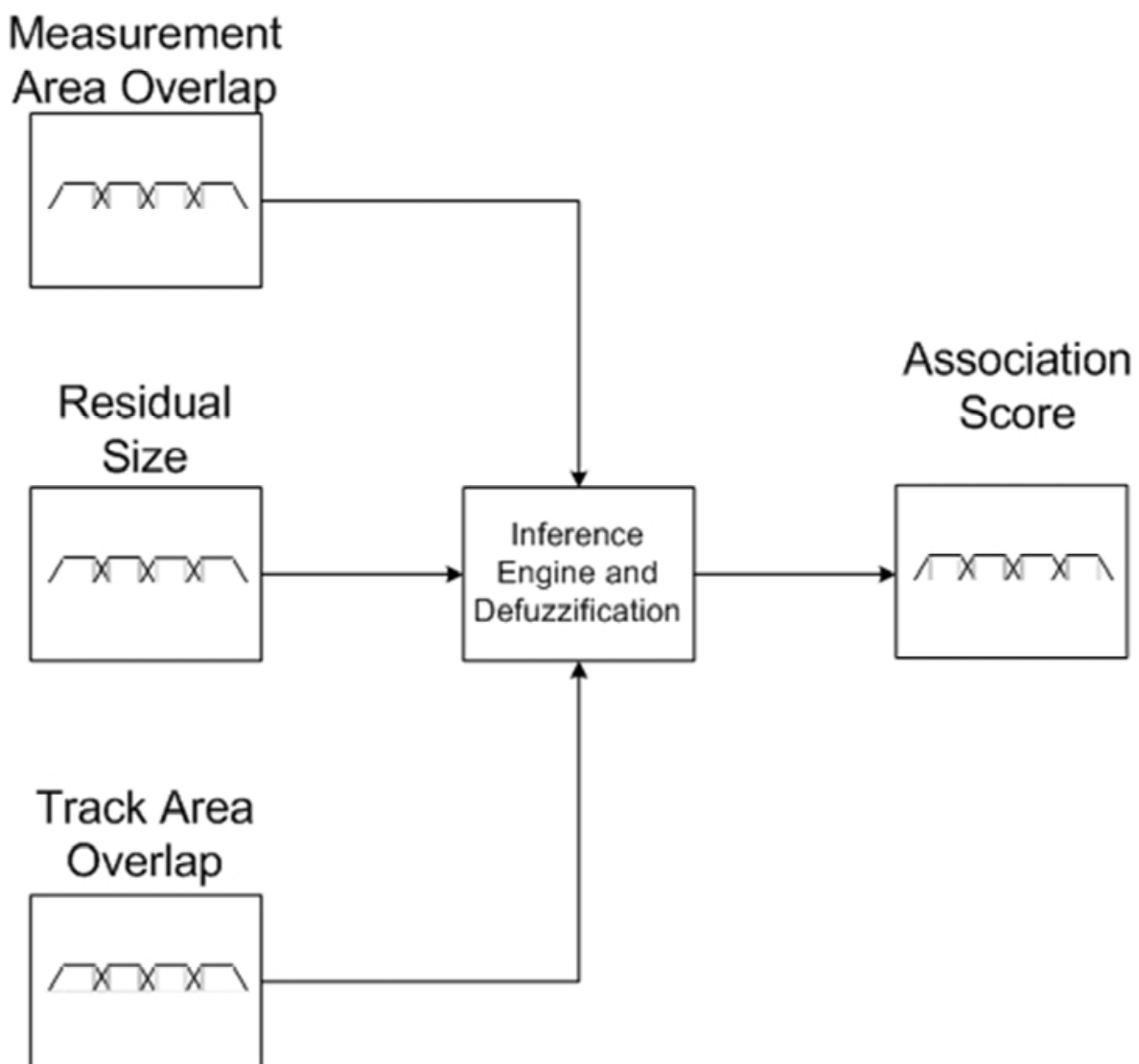


Fig. 6. Association score is generated using three inputs: overlap of the measurement uncertainty, overlap of the track uncertainty, and the residual size.

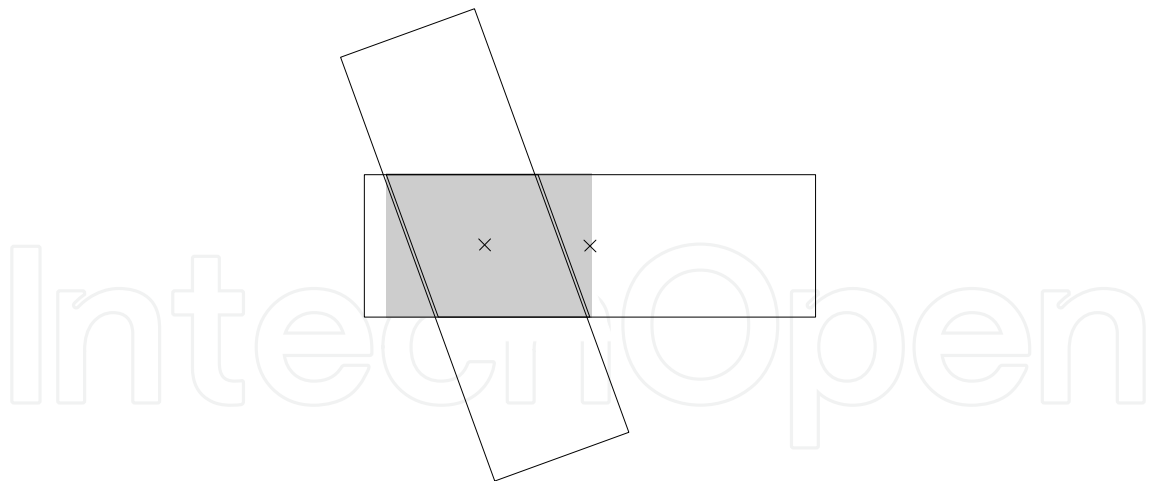


Fig. 7. Two uniform distributions show that overlap is the primary interpretation of their association.

The area of the overlapping region is compared to the possible percentage of overlap and a score is determined. The antecedent functions for each percentage is defined as shown in Figure 8.

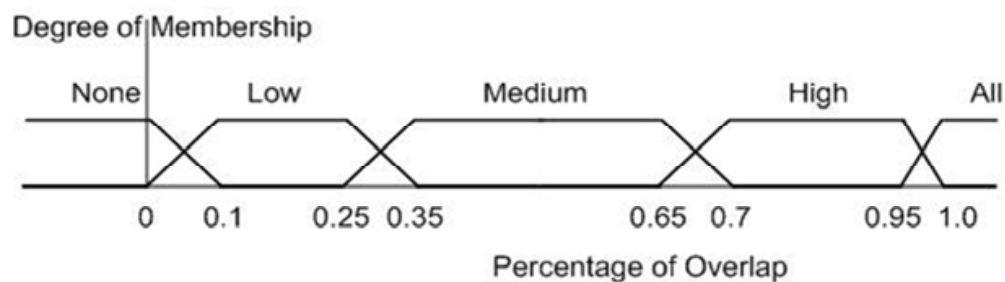


Fig. 8. Example antecedent functions

The consequence functions shown in Figure 9 are used to provide the association score.

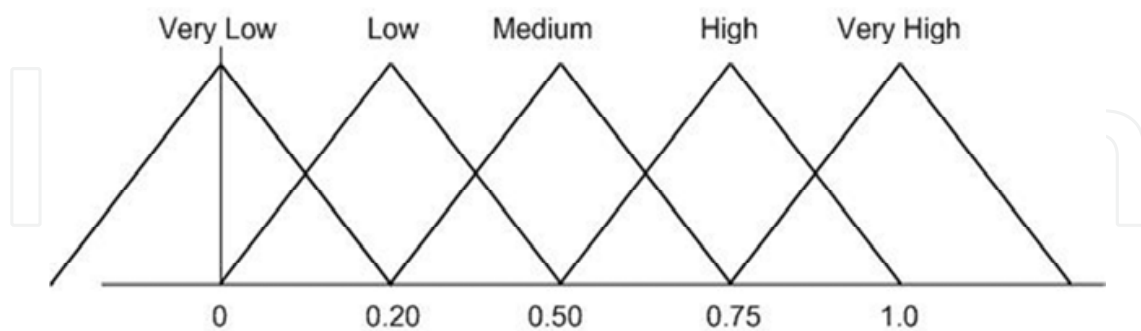


Fig. 9. Example consequence functions

In the second case, a Gaussian track and uniform measurement (or vice versa) was considered. The layered fuzzy logic approach with regards to the residual distance is again used to create the membership functions used to input information to the inference engine. The distance measure is the average distance from the Gaussian mean to the vertices of the uniform distribution and the mean of the uniform distribution. Figure 10 shows the distances used to form the measure for one example.

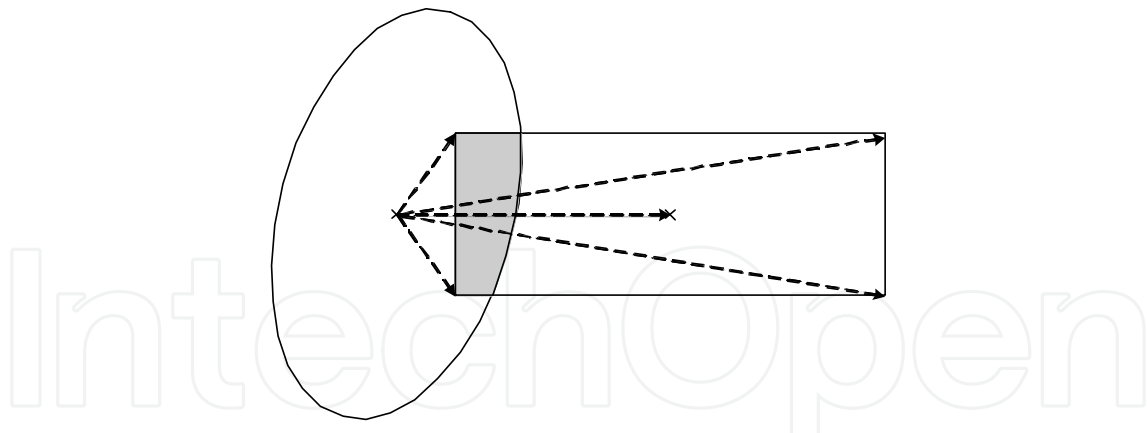


Fig. 10. Association of a Gaussian to a uniform distribution is dependent on both overlap and a modified residual.

The kinematic solution for fuzzy association was applied to other classes of probability density functions for research purposes. These efforts led to the concept of generating rule bases for different applications of association such as target classification and threat assessment. In these applications, the values can be discrete, continuous, or both. The associated uncertainties which are represented by the covariance matrix in the Gaussian representations often are not even measured values. For such applications, the use of fuzzy logic is quite effective. For the Level 1 target tracking application, classification is an important component of sensor reports and track description.

For classification information to be incorporated into the target track, the measurements can exist in two forms: target class and attribute information. For the target classification type measurements, two typical formats include a class and an associated quality score or a set of possible classes with associated probabilities (Pearl, 1988) or levels of evidence accrual (Stubberud, Kramer, and Geremia, 2007). For the former format, reports are provided similar to those exemplars listed in Table 1. The report is a pre-defined classification of the target. This is considered the measurement. The quality score can be a covariance as with Report 1, a probability as with Report 2, or generalized quality level as given with Report 3. The second reporting scheme provides a number of potential classes that the target may be, as seen in Table 2. Each possible class has an associated probability or degree of evidence. The reports look as a discrete probability density function. The probabilities should incorporate the quality in their generation. The evidence accrual results each have an associated quality score with them as shown in the table. In application, different classification algorithms have different methods of reporting results. Therefore, a centralized fusion system must be able to associate and combine the different reporting schemes. For target classification association, when the measurement reports are provided as a target class the fuzzy association scheme is implemented as seen in Figure 11.



Fig. 11. Classification Association Process Flow



Target	Class	Uncertainty/ Quality
1	2 (APC)	2.5
2	Tank	0.62
3	Truck	Good

Table 1. Exemplars of Classification Reporting Schemes and Their Uncertainties

Target Track #	Class 1 (Tank)	Class 2 (APC1)	Class 3 (APC2)	Class 4 (APC3)	Class 5 (Truck)
1	.1	.4	.3	.1	0
1 (Unc)	NA	NA	NA	NA	NA
2	.8	.5	.5	0	0
2 (Unc)	.01	.2	.01	0	0

Table 2. Exemplars of Probability and Evidence Accrual Based Reporting Schemes

The actual class is mapped through a fuzzy logic system to map the various classes into related values. For example, tank can be mapped into several values. Three such values are *armored vehicle*, *large vehicle*, and *tread vehicle*. An armored personnel carrier (APC) could map into *armored vehicle*, *medium vehicle* or *large vehicle*, and *tread vehicle* or *wheeled vehicle*. The fuzzy mapping would therefore a set of consequence membership functions for each value. These values then create a vector similar to the position and velocity vector for kinematics:

$$x_{class} = \begin{bmatrix} Tank \\ APC1 \\ APC2 \\ APC3 \\ APC4 \\ Truck \end{bmatrix} \quad (4)$$

The vector can be from one element to over a hundred elements that measure each attribute that various sensors can provide. The vector of the measurement and its counterpart for the target track then can create a residual vector

$$z_{class} = x_{class}^{Meas} - x_{class}^{Track} \quad (5)$$

Based on the different classification schemes six different reporting schemes exist as defined in Table 3. In each case, the following fuzzy logic association scheme is used as the basis with minor modifications in its implementation. Figure 12 shows the functional flow of this basis. As with the kinematic fuzzy association technique, the foundation is to use the Mahalanobis distance to build the algorithm. A residual of each classification vector exists from above. The next step is to generate a comparable uncertainty score. Unlike the Gaussian generation of the covariance, the score here will be a weighting,  $\mathbf{w}^{-1}$ , for the inner product

$$assoc\_score = z_{class}^T \mathbf{w}^{-1} z_{class} \quad (6)$$

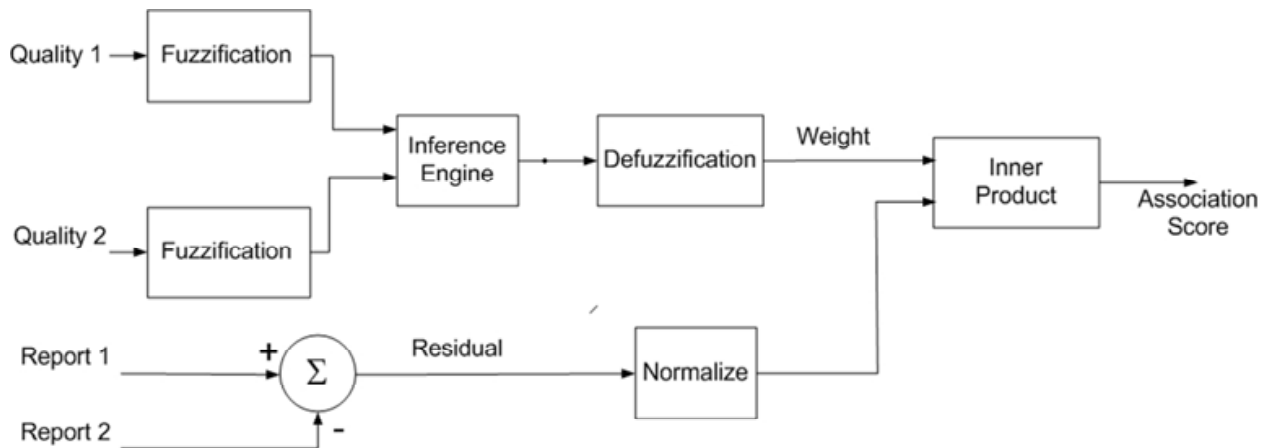


Fig. 12. Classification Uncertainty Association Incorporation

If the measurement or track is defined by a level of quality, the consequence membership function of Figure 13 is used. As with all previous defuzzification steps, the authors have used a center of gravity method. This is not a requirement but simply a preference. For evidence accrual technique, the associated covariance for the given class mapped to the consequence function using the antecedent membership function and the associated inference engine in Figure 14. The probability reports have a covariance set as a *good* covariance. The weighting score is generated using the fuzzy process defined in Figure 12.

Association	Report 1	Report 2
Type 1	Class/ Quality	Class/ Quality
Type 2	Class/ Quality	Probability
Type 3	Class/ Quality	Evidence
Type 4	Probability	Probability
Type 5	Probability	Evidence
Type 6	Evidence	Evidence

Table 3. Possible Association Combinations

For association Type 1 defined in Table 3, this is the process to compute the weight for Eq. (6) which is then the association score. For Type 2, the association score is generated for each potential class and multiplied by the probability of each class

$$\sum_{i=1}^{num\_class} p_i \cdot assoc\_score_i \tag{7}$$

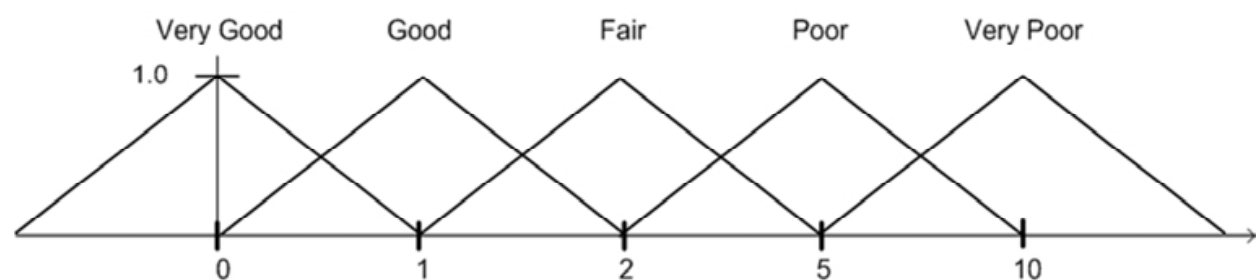


Fig. 13. Consequence Membership Function for Quality Mapping

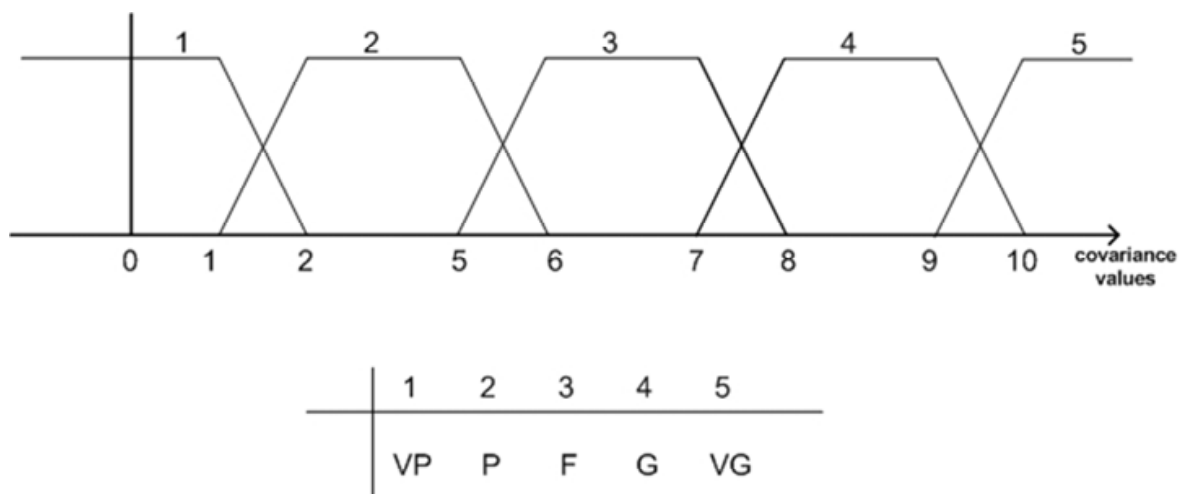


Fig. 14. Antecedent Function and Inference Engine for Numeric Quality Mapping

Type 3 is similar to Type 2 except that the probabilities used in Eq. (7) are replaced by a normalized evidence score for each class

$$p_i = \frac{e_i}{\sum_{i=1}^{num\_class} e_i} \quad (8)$$

Type 4 is generated by performing the association scores for each permutation and weighting them appropriately with the two sets of probabilities

$$\sum_{i=1}^{num\_class} \sum_{j=1}^{num\_class} p_j \cdot p_i \cdot assoc\_score_i \quad (9)$$

Type 5 replaces one set of probability scores from the Type 4 technique with one set of normalized evidence scores from Eq. (8). Type 6 association is the same as Type 4 association with the exception that the probabilities are replaced normalized evidence scores.

### 3. Optically inspired correlation

Optical computation is the process of using the physics of light, lenses, and filters to provide specific computations at the fastest speeds possible, the speed of light. By modeling light's behavior with mathematical functions, these functions can be performed on dedicated hardware platforms. One such function is that of optical correlation (Kumar, Mahalanobis, and Juday, 2005). The process is shown in Figure 15.

Coherent light is passed through a thin film Red-Green-Blue (RGB) screen called a spatial light modulator (SLM). On one of the set of pixels (assume Red) or channel, an image is placed. The coherent light projects this image through lens onto a second SLM. The new image is the two-dimensional (2D) Fourier transform or fast Fourier transform (FFT) of the image on the first SLM. On the second channel, the 2D-FFT of a comparison image is placed and the pixels are individually multiplied. The resulting multiplied image is placed in the third channel and projected by the coherent light through a second lens onto a third lens. This provides the inverse 2D-FFT of the combined image which is actually the correlation

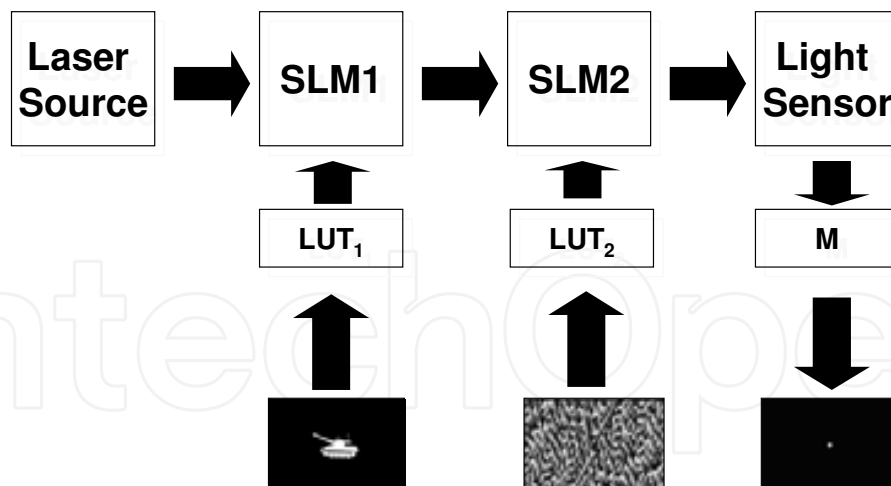


Fig. 15. Optical correlation functional flow using an optical correlation device.

function. (This will be mathematically described below.) For clarity, the input image at the first SLM will be the measured or test image. The image whose 2D-FFT is placed at the second SLM is the reference image. As seen in Figure 16, if the reference image is centered when transformed so that the correlation peak will be centered about the location of the reference image in the test image. In the case of Figure 16, two copies of the reference image exist in the test image and, thus, two correlation peaks exist. Both are centered about their locations in the test image. This implies that optical correlation can be used for both fast processing and parallel processing (multiple correlation comparisons simultaneously).

One problem with the optical correlator is that the SLMs limit the range of values that the image amplitude can attain. The pixels are integer values between 0 and 255. The image at the last SLM is only the real part of the final transform. Also, in some optical correlators, the amplitude of the test image's 2D-FFT is normalized to 1, (Kumar, Mahalanobis, and Juday, 2005). This is a physical limitation in optical correlators, especially early versions. The normalization of amplitude implied that only the phase information was used. Despite this apparent limitation, this so-called phase-only filter has actually provided improved correlation results.

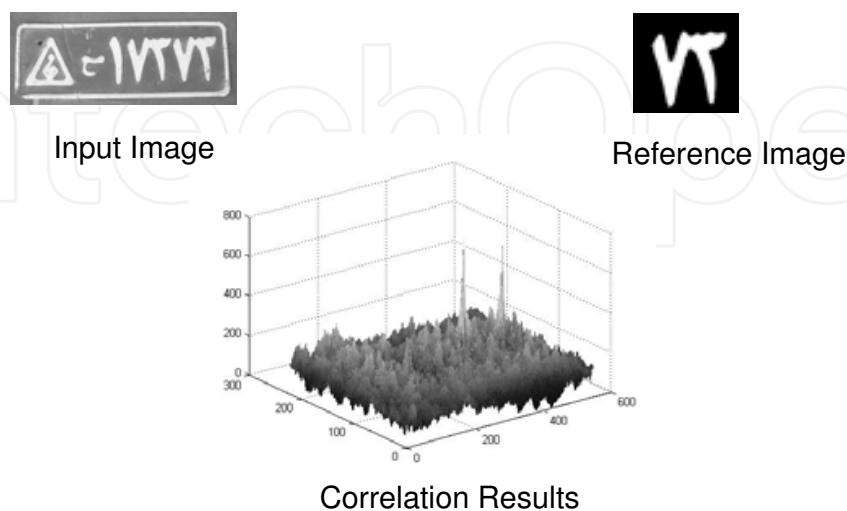


Fig. 16. Two correlation peaks are created aligned with the location of the reference image in the input image.

The mathematics of the optical physics is straightforward. The standard correlation function between two images  $\mathbf{F}$  and  $\mathbf{G}$ , is defined as

$$\begin{aligned} & \sum \sum f^*(x,y) f(x+X,y+Y) \\ &= \sum \sum F^*(k_x,k_y) F(k_x,k_y) e^{-j(k_x X+k_y Y)} \\ &= \mathfrak{I}^{-1} \left\{ \left| F(k_x,k_y) \right|^2 \right\} \end{aligned} \quad (3)$$

As in basic signal processing (Oppenheim, Willisky, and Hamid, 1996), the spatial or time domain can be computed using frequency domain techniques. The frequency domain version of the correlation function is defined as

$$\begin{aligned} & \sum \sum g^*(x,y) f(x+X,y+Y) \\ &= \sum \sum G^*(k_x,k_y) F(k_x,k_y) e^{-j(k_x X+k_y Y)} \\ &= \text{Re} \left\{ \mathfrak{I}^{-1} \left\{ G^*(k_x,k_y) F(k_x,k_y) \right\} \right\} \end{aligned} \quad (4)$$

where  $F$  is the Fourier transform. With amplitude information normalized, the POF form of the correlation function based on the optics is

$$\begin{aligned} & \sum \sum G^*(k_x,k_y) \frac{F(k_x,k_y)}{|F(k_x,k_y)|} e^{-j(k_x X+k_y Y)} \\ &= \text{Re} \left\{ \mathfrak{I}^{-1} \left\{ G^*(k_x,k_y) \frac{F(k_x,k_y)}{|F(k_x,k_y)|} \right\} \right\} \end{aligned} \quad (5)$$

With the advent of faster computers and the desire to avoid using specialized hardware, the optical correlator is rarely used but the mathematics of the optical physics provides a powerful tool for the correlation problem which can be applied to the data fusion association problem.

### 3.1 Amplitude tile

For the Level 1 fusion problem, the image used for correlation is referred as a tile. The tile is a two-dimensional image that maps data about the target track and the measurement reports into an amplitude plot. Figure 17 presents an example of a amplitude tile. In this case, the tile is 50 x 200 pixel image. The attributes of the target track vector or the measurement vector are the vertical components. The horizontal components are the time reports. Each 10 x 10 block represents a given attribute at a given time. The rows or attributes are defined as:

- target latitude
- target longitude
- target altitude
- target speed

- target course heading
- target classification

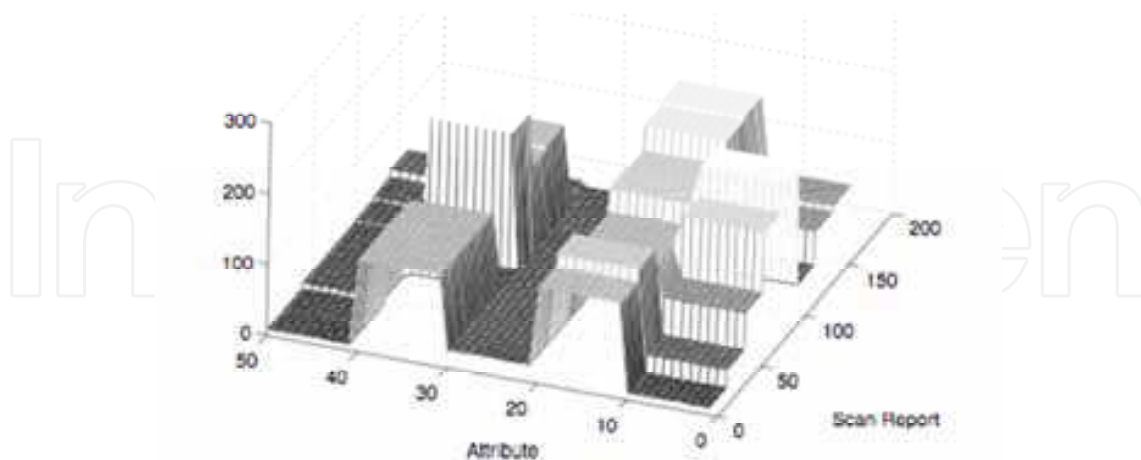


Fig. 17. The amplitude tile creates blocks valued between 0 and 255.

The columns are these attributes at different times. For amplitude tile, the intensity of each 10x10 block is a value between 0 and 255. The range of values for position is limited by the region of interest. This implies that, if the region of interest is for air targets between latitude 32°N and 40°N and 25°E and 33°E, each degree change for latitude the intensity would change by 31.875 in amplitude as would each change in intensity for longitude. Similar ranges could be created for the other attributes.

### 3.2 Phase tile

The image tiles can be created in a different format. This second 10x10 block format is that each pixel of the (m,n)<sup>th</sup> block is generated by

$$\sin(\omega_m i_{mn} + \phi_{mn}) \cdot \sin(\omega_n j_{mn} + \phi_{mn})$$

where  $m$  is the number of attributes and  $n$  is the number of time steps. The values of  $i$  and  $j$  represent the individual pixel within the 10x10 block. An example of a tile from this phase generation is shown in Figure 18.

The phase variations range between 0 and 180 degrees depending on the attribute value. The selection of the phase would be made similar to the amplitude change above. Each attribute has its own frequency as well. This is done to separate each attribute more clearly in the frequency domain.

## 4. Image-based association with uncertainty and classification information

The image correlation technique, described in Section 3, has been demonstrated to work comparably to the techniques that use the chi-squared metric based on the Mahalanobis distance (Stubberud and Kramer, 2010a) and (Stubberud and Kramer, 2009). The incorporation of uncertainty into the algorithm began with the use of a sample set of points in the uncertainty ellipse (Stubberud and Kramer, 2010b). An iterative process of association scores were generated and weighted similar to the technique that was developed in this chapter for the fuzzy logic association applied to the classification problems where evidence or probabilities described the measurement. The technique is easily extended to uniform

distributions as well as other distributions. In this section, an uncertainty model is introduced that remaps the phase distribution for the uncertainty model using fuzzy logic techniques derived from the methods of Section 2. The section concludes with the incorporation of classification information where the Gaussian assumption is not valid.

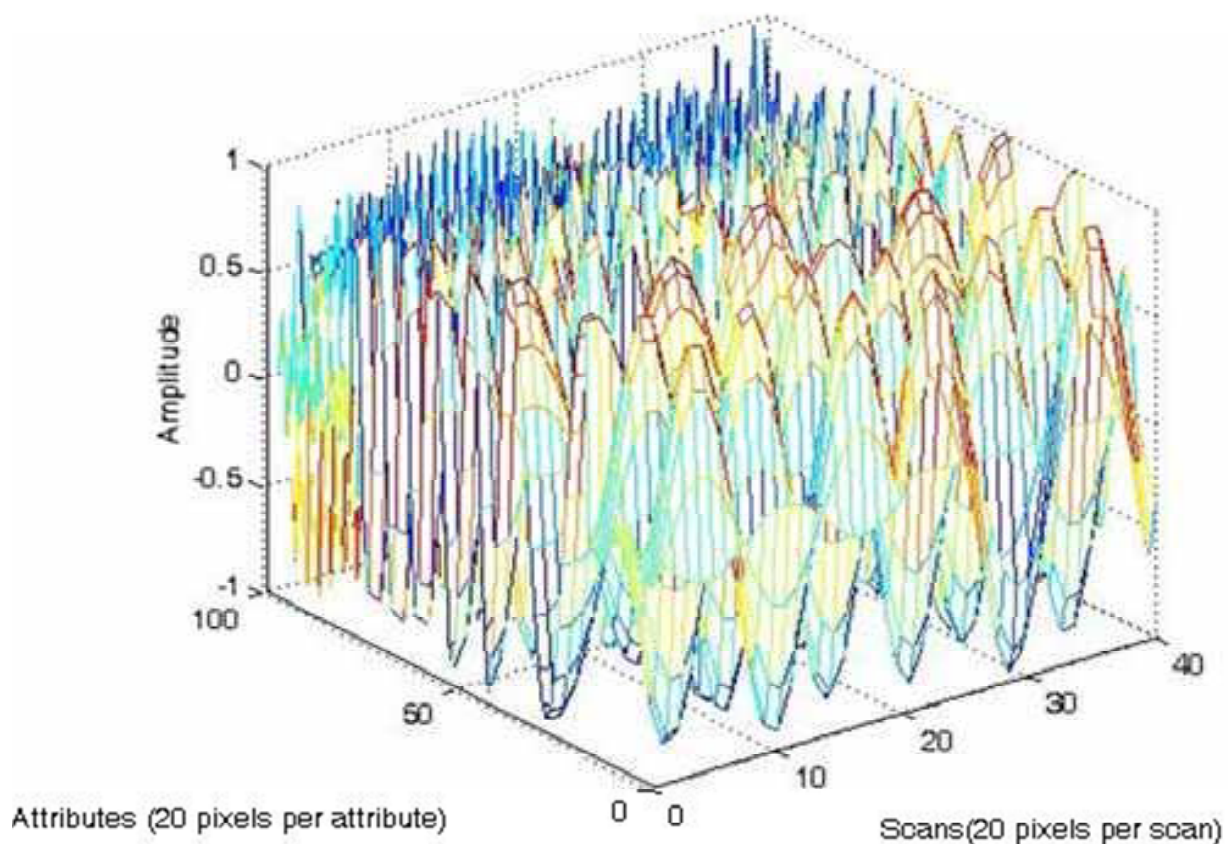


Fig. 18 The phase tile maps sinusoids with phases between 0 and 180 degrees.

#### 4.1 Fuzzy logic applied to phase variation for tile generation

In (Stubberud and Kramer, 2009) a fuzzy logic approach to the data association problem was developed. There, the technique used multi-layered fuzzy logic to create a score by implementing a linguistic interpretation of the chi-squared metric. Closeness was based on the weighted distance between the two track elements. It also considered the overlap of the error ellipses. In this approach, a similar view of the error ellipses is used. Instead of using complex mathematical distances which would be adverse to the simplicity of the image correlation technique, a basic fuzzy logic approach is developed to adjust the tile creation based on the uncertainty ellipse size and orientation.

The first variable to be mapped is that of the orientation of the error ellipses. The fuzzy memberships are defined as five potential angles of the error ellipse relative to the longitude (x-axis). As seen in Figure 19, the memberships are  $0^\circ$ ,  $45^\circ$ ,  $90^\circ$ ,  $135^\circ$ ,  $180^\circ$ . The alignments provide two inputs to the fuzzy decision process described in Figure 20. The first is a weighting factor that is generated using the crisp value of the antecedent functions. These weights are used in the defuzzification process of the second defuzzification step in Figure 20. The second input is the different rules that are activated from the inference engines in

Tables 4 and 5 which relate to longitude component of the target track (or the x-axis) or the latitude component of the track (x-axis). These rules from the first stage determine vary the inputs to the inference engine the second stage (Table 6). The variations in the inputs are defined in Table 7. The input A indicates the average size of the minor or major axes of the uncertainty ellipse of Track 1 and B indicates the average of minor or major axes of Track 2. The table also indicates that multiple instantiations of the fuzzy inference engine are used in several cases.

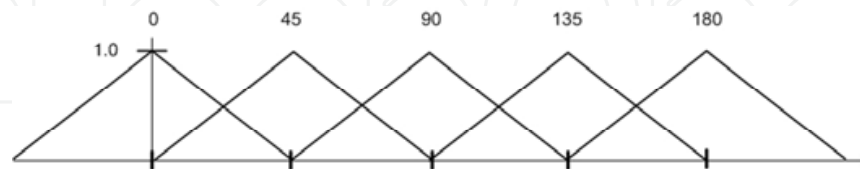


Fig. 19. The antecedent triangular membership functions used to determine the alignment of the uncertainty ellipses.

Degrees Longitude	0	45	90	135	180
Effect	1	2	3	2	1

Table 4. Inference Engine Major Axis Alignment of Covariance Effect on Longitude (x-axis)

Degrees Latitude	0	45	90	135	180
Effect	3	2	1	2	3

Table 5. Inference Engine Major Axis Alignment of Covariance Effect on Latitude (y-axis)

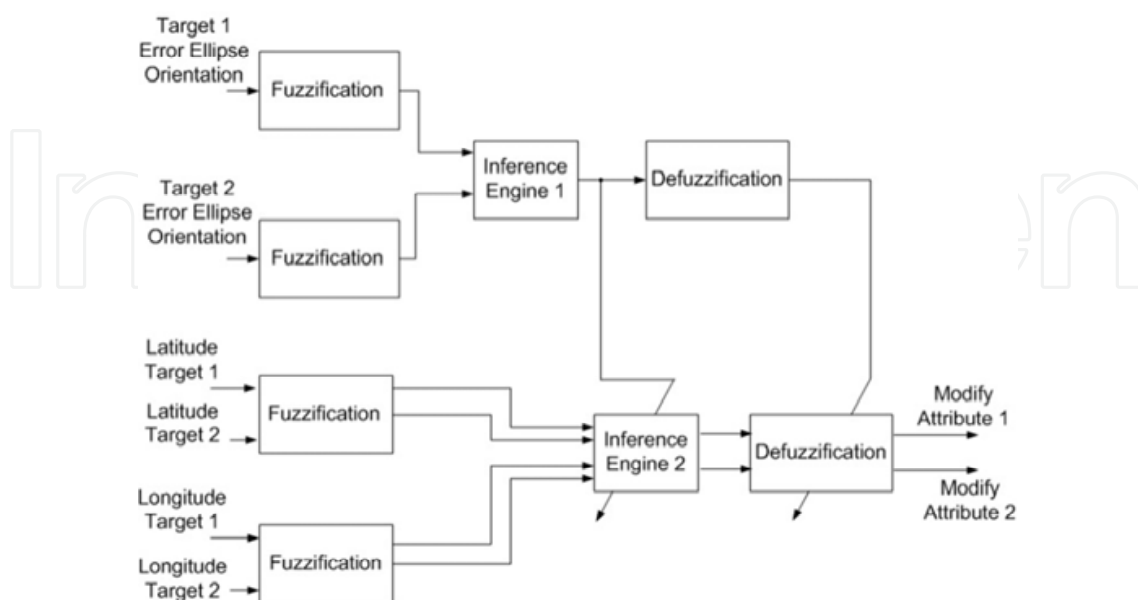


Fig. 20. The fuzzy logic process to vary the tile generation used in image correlation track association process.



		B			
		Small	Medium1	Medium2	Large
A	Small	1	2	3	4
	Medium1	2	3	4	5
	Medium2	3	4	5	6
	Large	4	5	6	7

Table 6. Inference Engine of Averaged Aligned Error Covariance Axis Sizes

The second process is based on the size of the axis of interest of the uncertainty ellipse. The actual uncertainty in the directions of latitude and longitude are mapped to membership functions in Figure 21. The elements of the membership functions are small, medium\_one, medium\_two, and large. Since the uncertainty measure is global, i.e., averaged over the entire time window, the results will affect all of the time subtiles of the entire attribute similarly. The proposed inference engine, defined in Table 4, vary depending on the alignment rule from the first step. If multiple instantiations are desired, then the output of each instantiation is weighted by the noted factor in Table 5. An NA indicates that those rules are not used and result in a zero value for that component.

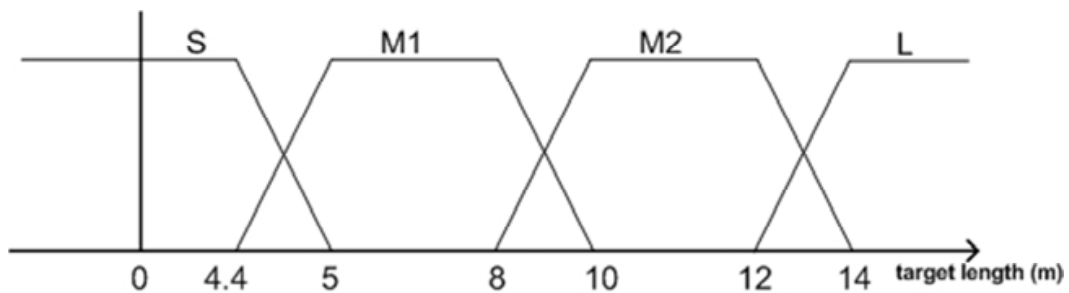


Fig. 21. The antecedent triangular membership functions used to determine the size of the uncertainty ellipses axis.

Alignment			Component							
T1	T2	Wt.	A1	B1	A2	B2	A3	B3	A4	B4
1	1	1	Maj	Maj	NA	NA	NA	NA	NA	NA
1	2	0.5	Maj	Min	Maj	Min	NA	NA	NA	NA
1	3	1	Maj	Min	NA	NA	NA	NA	NA	NA
2	1	0.5	Maj	Maj	Maj	Maj	NA	NA	NA	NA
2	2	0.25	Maj	Maj	Maj	Min	Min	Maj	Min	Min
2	3	0.5	Maj	Min	Min	Min	NA	NA	NA	NA
3	1	1	Min	Maj	NA	NA	NA	NA	NA	NA
3	2	0.5	Min	Maj	Min	Min	NA	NA	NA	NA
3	3	1	Min	Min	NA	NA	NA	NA	NA	NA

Table 7. Alignment Effects on the Covariance Inference Engine and Process

To simplify the development in this paper, the association score is generated on only the position data. The extension to include velocity is simply to repeat the process on the velocity measures and uncertainties.

The consequence function is the same as that seen in Figure 22. The defuzzified value is used to reduce the phase range.

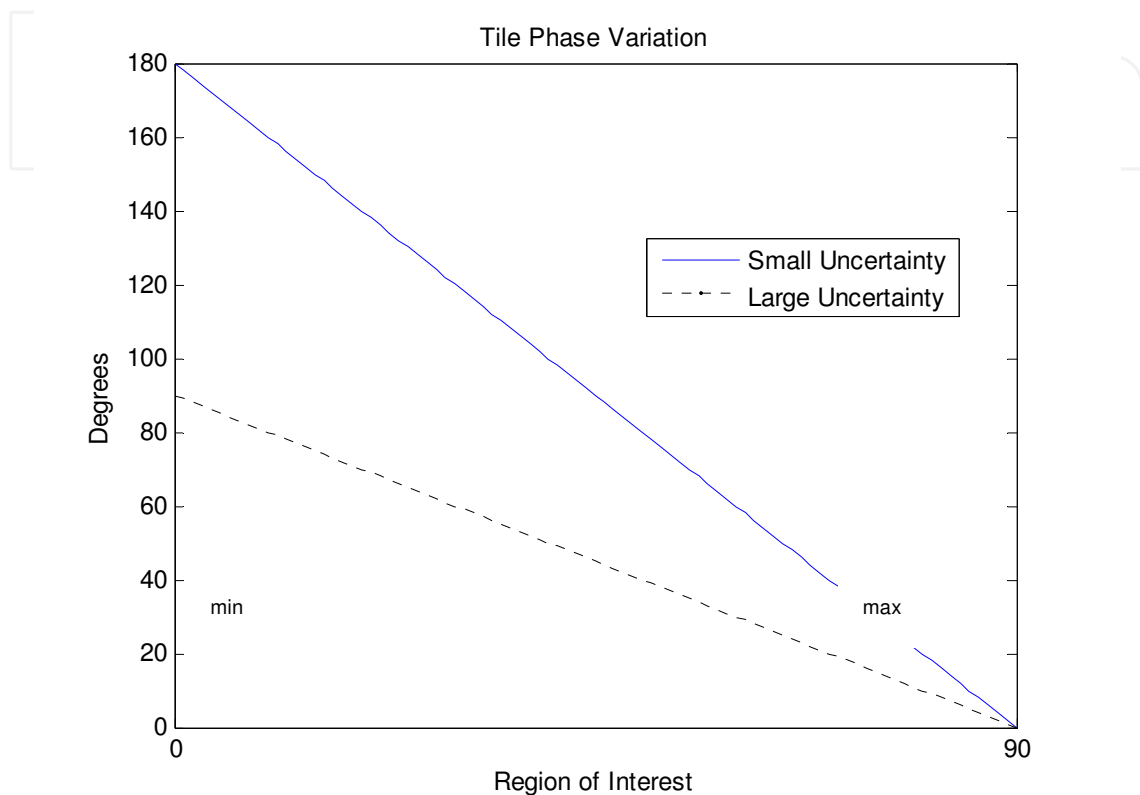


Fig. 22. An Example of the Change in Range of the Phase Variation Based on Track Uncertainty.

#### 4.1.1 Incorporating uncertainty as a quantization of the phase separation

To vary the phase difference in generating the subtiles using uncertainty, at each time instance, an estimate of the effects of both track's uncertainty on the association score is made. For each attribute, a modification score using the fuzzy logic process described in Section 4 is made. This modification score is computed for each attribute at each report time or scan for both tracks.

The modification score changes the range of phase values used to adjust the phase of each attributes value. As seen in Figure 22, the linear range of values is reduced as the uncertainty becomes larger. The nominal range is from  $0^\circ$  to  $180^\circ$ . As the range shrinks the variation in the phase for changes becomes less. As would be the case with the chi-squared metric, larger differences can be tolerated.

#### 4.1.2 Example and results

To analyze the performance of the new image-correlation association that incorporates uncertainty, a scenario with two targets and four sensor systems was generated to compare

the incorporation of uncertainty in a global manner to image-correlation data association routine. The two targets' trajectories are depicted in Figure 23.

The target on top is considered Target 2. The three sensors platforms, which are stationary throughout the scenario, are also shown. The sensors are identical range-bearing sensors, i.e., a radar or active sonar, each with Kalman filter kinetic target tracking systems on them. The association scores are generated to compare the position-only data form each track from the first three sensor systems.

Figure 24 depicts the difference between the track of Target 2 from both Sensor 1 and Sensor 3 and the track for Target 1 from Sensor 1. In Figure 25, the association scores between the two tracks of Target 2 are shown for the original image-correlation technique without uncertainty and the new uncertainty-incorporation method.

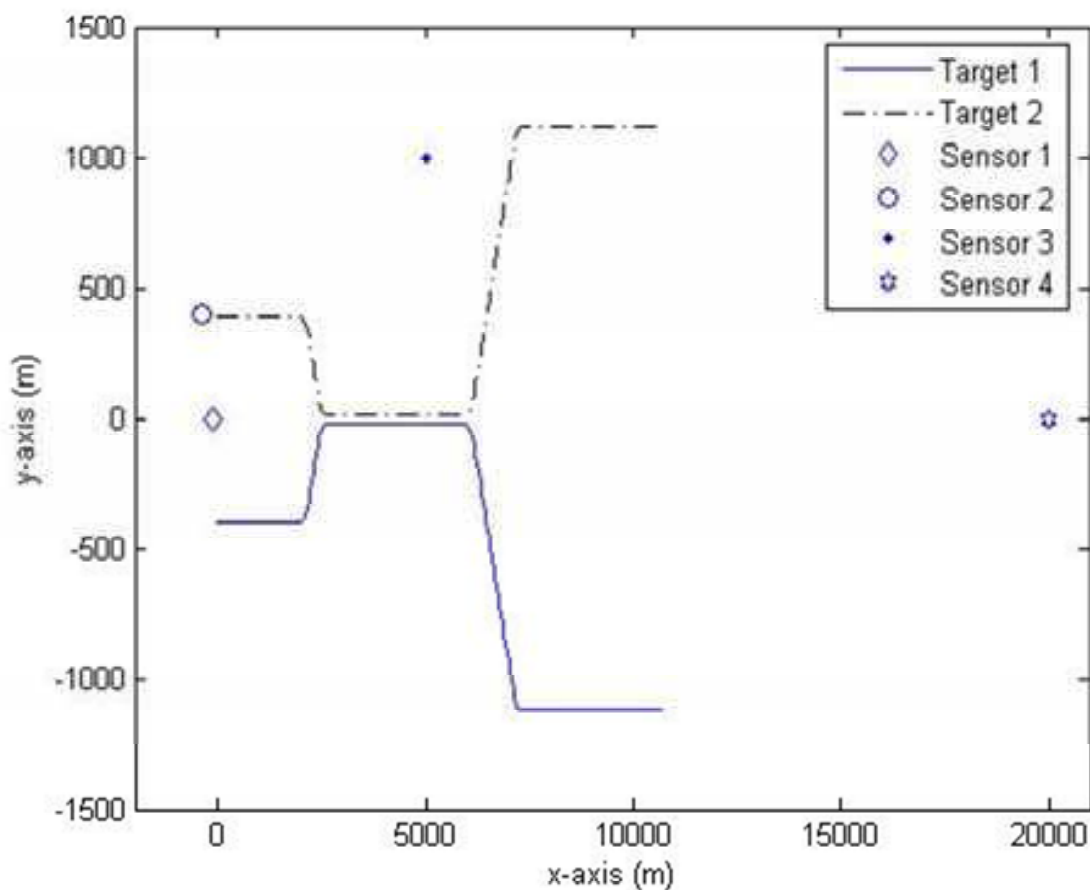


Fig. 23. Two target example scenario.

The incorporation of uncertainty reduces the variation in the scores. This is a benefit of the use of uncertainty similar to the chi-squared metric. Also, the uncertainty method reduces the loss of association score as the target gets further from the sensors. A similar comparison of the association scores for both techniques between Sensor 1's Target 1 track and Sensor 3's Target 2 track is shown in Figure 26. In this comparison, the uncertainty association does better in that it produces lower scores for the differences between the positions of the target tracks.

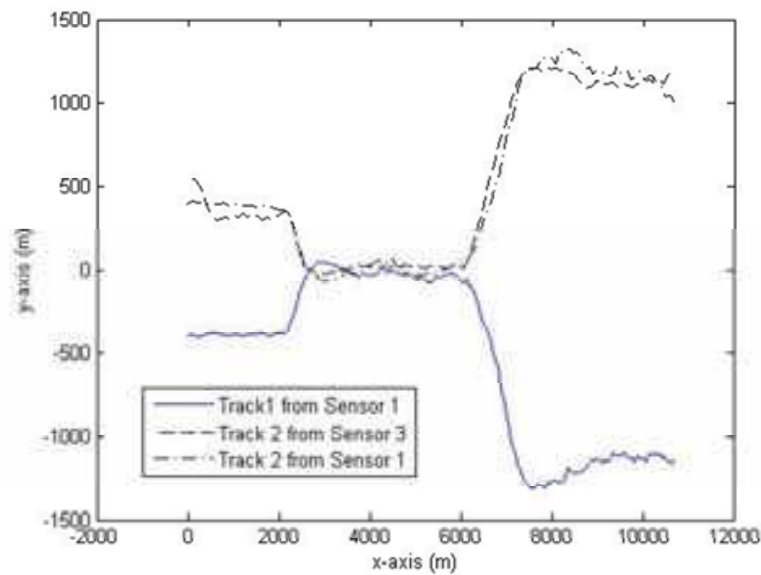


Fig. 24. Track results for Target 1 and Target 2 for Sensor 1 compared to track results for Target 2 for Sensor 3.

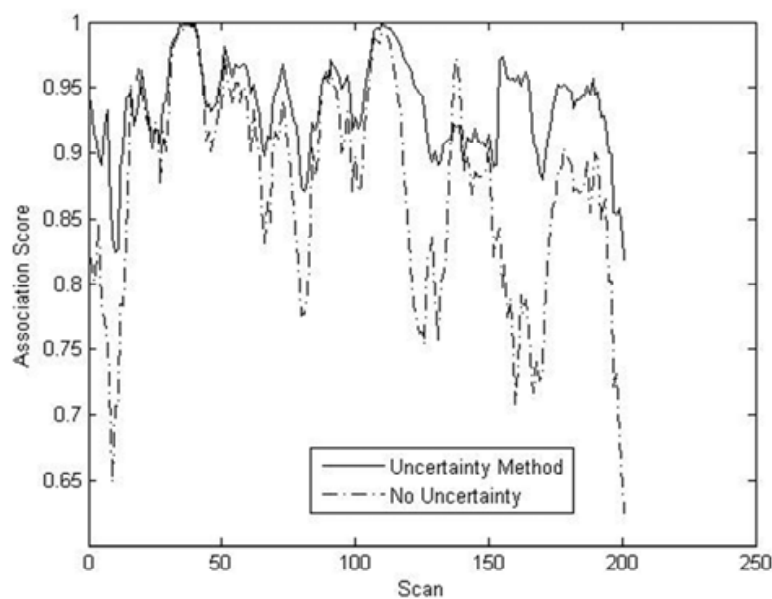


Fig. 25. Association score comparison of results with and without incorporation of uncertainty.

Figure 27 provides a more detailed analysis of uncertainty association scores of the tracks for Target 2 from Sensor 1 and Sensor 3. The reports of Scan 10 and Scan 195 are marked. By comparing the results to the actual tracks seen in Figure 26, it is apparent that the scores follow the differences in the tracks. At Scan 10, a full tile is generated for the first. (Prior to this, ten scans of data for each attribute were not available.) At the tenth scan, the target tracks were separated in position in the y-coordinate of the first leg of the trajectory. Since the sensors were fairly close to the targets, the uncertainty was “small” and, therefore, the association score became poor. For the most part after that, the association score settled near

or above 0.9 until the end. By this time, around Scan 195, the uncertainty from both tracks started to become more aligned. This means that the small range error would bring the x-coordinate uncertainty in the track down. The x-coordinate lag Sensor 1's track seen in the last two legs of the Target 2 trajectory now have a greater impact on the score. This drives the association score downwards.

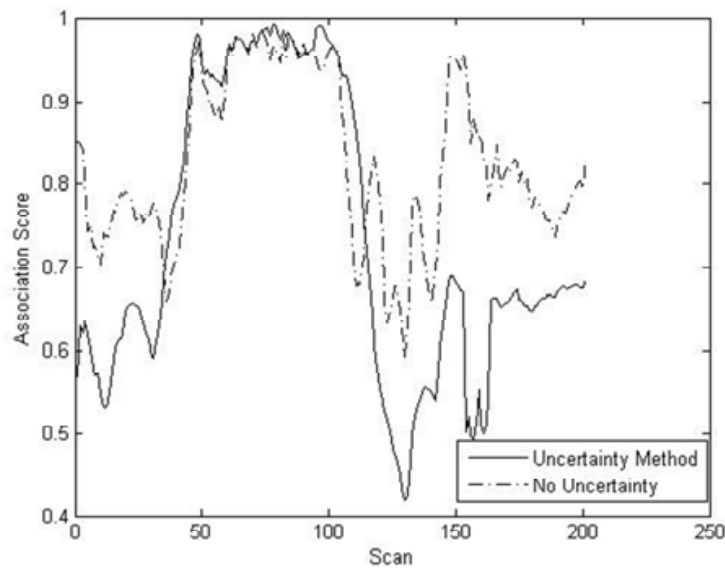


Fig. 26. Association score comparison of results with and without incorporation of uncertainty.

#### 4.2 Incorporating classification into image-based association

The incorporation of classification is a two-step process. The first step is the definition of the new attributes for the tile. The second is the incorporation of uncertainty.

In Section 2, the classification of a target was mapped into a set of subclasses and those were mapped into numeric values using fuzzy logic. In this development, a similar approach is used. The use of the subclasses creates more attributes for the tile generation. As with the exemplar above, three attributes are used for each class *armor\_type*, *wheel/tread*, and *vehicle\_size*. Each attribute would have a 20x20 pixel subtile for each scan or report of data. Each class would be set to its own phase predetermined by the nearness of the relationship. Thus, as seen in Table 8, a number phase differences vary based on their relationships to each other.

To incorporate uncertainty, two techniques are used. The first is the probability of an attribute. In the example, and a generic APC can be either a wheeled or tread vehicle. If the specific type of APC is not know then a probability of either type would exist. For example, assume there is a 0,6 probability that an APC would have a tread. The subtile would then have 12 pixels of its horizontal set to tread while 8 pixels would be set as wheeled (see Figure 28). Every change as the classification information becomes better would change the composition of the subtile for the given scan as further shown in Figure 28 The quality uncertainty of each report would then be generated using the redistribution of the phases by shrinking or expanding the range of values in Table 8 using the technique described in Section 4.1. For example, a large uncertainty (or poor quality) measurement/ track pair would have phase ranges similar to those in Table 9.

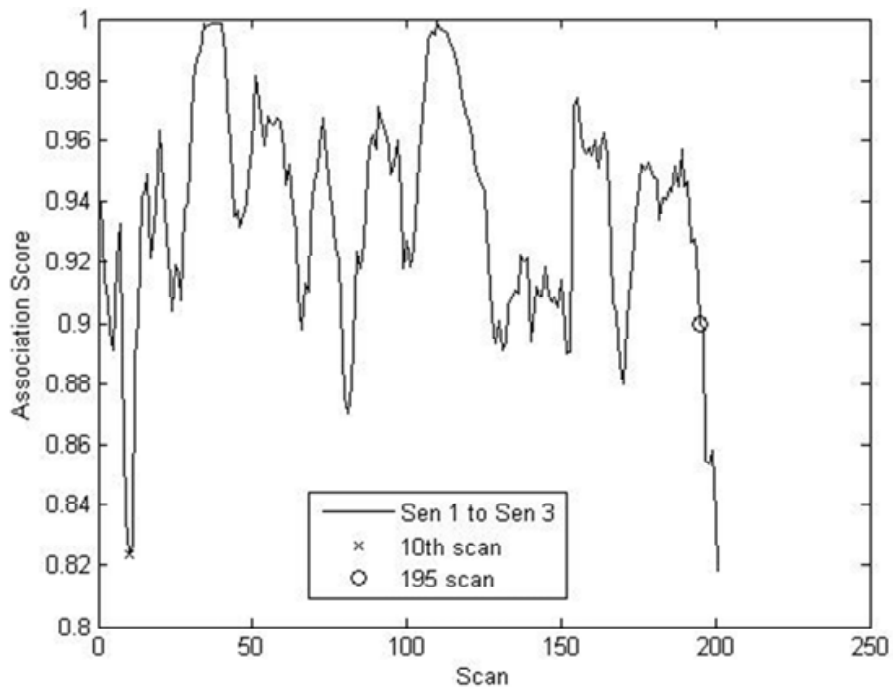


Fig. 27. Association scores using the uncertainty method for the tracks for Target 2 from Sensor 1 and Sensor3

Class	Attribute Phase Value (degrees)			
	Val. 1	Val. 2	Val. 3	Val.4
Armor_Type	0	45	170	NA
Wheel/ Tread	0	180	NA	NA
Vehicle_Size	0	10	45	90

Table 8. Classification Attribute Mapping To Phase Differences

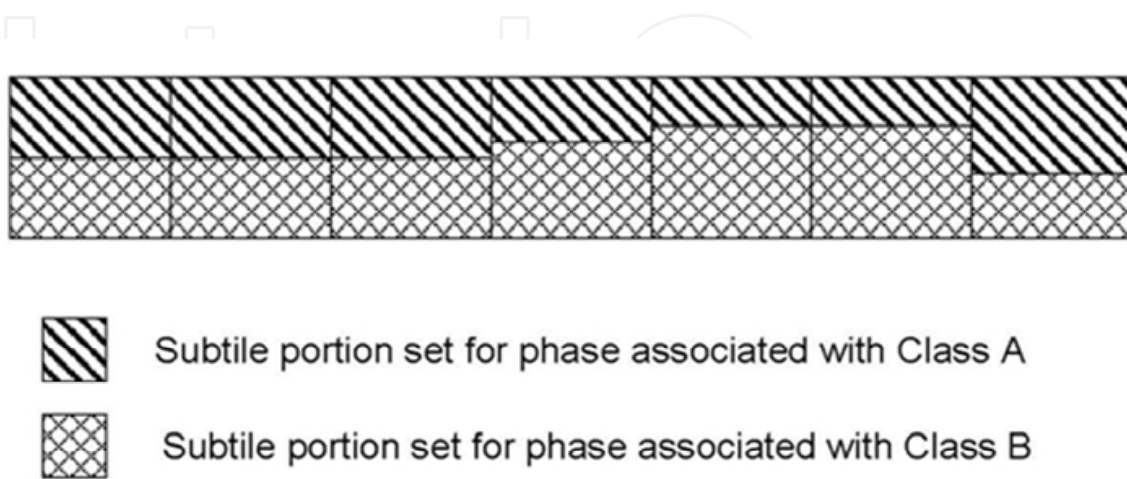


Fig. 28. Subtile separation based on probability score of different attributes.

Class	Attribute Phase Value (degrees)			
	Val. 1	Val. 2	Val. 3	Val. 4
Armor_Type	0	12	90	NA
Wheel/ Tread	0	45	NA	NA
Vehicle_Size	0	5	20	45

Table 9. Classification Attribute Mapping To Phase Differences With Large Uncertainties

#### 4.2.1 Example and results

The aforementioned example from Section 4.1.2 is again used. In this problem, the target classification is given as in Table 10 for the measurement and the track. The table details probability for each of the element of the attribute. The results of the classification algorithm for Target 2 from Sensor 1 and Sensor 3 are shown in Table 11. The classification differences have significant impact on the association scores as expected.

Class (Target #)	Report (Uncertainty)										
	1 (.3)	1 (.2)	1 (.2)	1 (.2)	1 (.2)	1 (.2)	1 (.2)	1 (.2)	1 (.2)	1 (.2)	1 (.2)
Armor_Type (1)	1 (.3)	1 (.2)	1 (.2)	1 (.2)	1 (.2)	1 (.2)	1 (.2)	1 (.2)	1 (.2)	1 (.2)	1 (.2)
Wheel/ Tread (1)	1 (7)	2 (7)	2 (6.5)	2 (6.8)	1 (6.9)	1 (6.4)	1 (6.2)	1 (6.1)	2 (6.4)	2 (6.5)	1 (6.6)
Vehicle_Size (1)	1 (2.3)	1 (2.2)	1 (2.2)	1 (2.1)	1 (2)	1 (1.9)	1 (1.9)	1 (2)	1 (1.8)	1 (1.8)	1 (1.7)
Armor_Type (2)	2 (.3)	2 (.2)	2 (.2)	2 (.2)	2 (.2)	2 (.2)	2 (.2)	2 (.2)	2 (.2)	2 (.2)	2 (.2)
Wheel/ Tread (2)	2 (7)	2 (6.4)	2 (6.4)	2 (6.4)	2 (6.4)	1 (6.4)	2 (6.4)	1 (6.4)	2 (6.4)	2 (6.4)	2 (6.4)
Vehicle_Size (2)	2 (2.3)	2 (2.3)	2 (2.4)	3 (2.7)	3 (2.8)	3 (2.9)	2 (2.7)	2 (2.6)	2 (2.5)	1 (2.8)	2 (2.9)

Table 10. Classification Reports For Target 2/ Sensor 1 And Target 2/ Sensor 3

Association Score			
Scan 8	Scan 9	Scan 10	Scan 11
0.59	0.56	0.56	0.52

Table 11. Association Score Between Target 2/ Sensor 1 and Target 2/ Sensor2

## 5. Conclusion

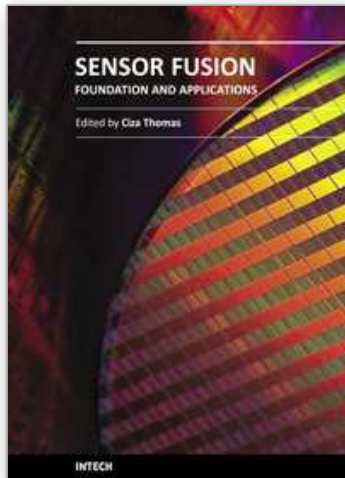
The use of Gaussian distribution in target tracking is becoming less prevalent than in the past. New association techniques are needed for the fusion process. The approaches need to look at previously unused technologies or techniques used for other applications in the past. In this chapter, new techniques for data association were addressed and applied to current fusion problems that combine kinematics and classification as well as address non-Gaussian uncertainty measures.

## 6. References

- Alspach, D.L., A Bayesian Approximation Technique for Estimation and Control of Time Discrete Stochastic Systems, Ph.D. Dissertation, University of California San Diego, 1970.
- Alspach, D. & Sorenson, H., (1972). "Nonlinear Bayesian Estimation Using Gaussian Sum Approximations," *IEEE Transactions on Automatic Control*, Vol. 17, No. 4, pp. 439 – 448, Aug., 1972.
- Arulampalam, M.S., Maskell, S., Gordon, N., and Clapp, T. (2002). A Tutorial on Particle Filters for Online Nonlinear/ Non-Gaussian Bayesian Tracking, *IEEE Transactions on Signal Processing*, Vol. 50, No. 2, (February 2002), pp. 174 – 188, ISSN: 1053-5872
- Blackman, S. (1986). Multiple-Target Tracking with Radar Applications, Artech House, ISBN 0890061793, Norwood, MA, USA
- Brown, R.G. (1983). Introduction to Random Signal Analysis and Kalman Filtering, John Wiley and Sons, ISBN: 978-0471087328, New York, NY, USA
- Dempster, A. (1967). Upper and Lower Probabilities Induced by a Multivalued Mapping, *Annals of Mathematical Statistics*, Vol. 38, No. 2, (April 1967), pp. 325 – 339, ISSN 0003-4851
- Haykin, S. (2002). Kalman Filtering and Neural Networks, Prentice-Hall, ISBN 0471369985, Englewood Cliffs, NJ, USA
- Blackman, S. (1986). Multiple-Target Tracking with Radar Applications, Artech House, ISBN 0890061793, Norwood, MA, USA
- Kosko, B. (1992). Neural Networks and Fuzzy Systems: A Dynamical Systems Approach to Machine Intelligence, Prentice Hall, ISBN 0136114350, Englewood Cliffs, New Jersey, USA
- Kumar, B.V.K.V., Mahalanobis, A., and Juday, R.D. (2005). Correlation Pattern Recognition, Cambridge University Press, ISBN:0-521-57103-0, Cambridge, UK
- Llinas, J.; Bowman C.; Rogova, G.L.; Steinberg, A.; Waltz, E. & White, F. (2004). Revisions and Extensions to the JDL Data Fusion Model II, Proceedings of Fusion 2004, pp.1218-1230, ISBN 91-7056-117-6, Stockholm, Sweden, July 2004.
- Mahalanobis, P C (1936). On the Generalised Distance in Statistics, Proceedings of the National Institute of Sciences of India, Vol. 2, No. 1, pp. 49–55.
- Oppenheim, A.V., Willsky, A.S., and Hamid, S. (1996). Signals and Systems, 2nd Edition, Prentice Hall, ISBN: 9780138147570, Upper Saddle River, NJ, USA
- Pearl, J (1988). Probabilistic Reasoning in Intelligent Systems: Networks of Plausible Inference, Morgan Kaufmann Publishers, ISBN 1558604790, San Mateo, CA, USA
- Shafer, G. (1976). A Mathematical Theory of Evidence, Princeton University Press, ISBN 978-0691100425, Princeton, N.J, USA



- Shea P.J, Zadra, T., Klamer, D., Frangione, E., Brouillard, R. and Kastella, K. (2000). Precision Tracking of Ground Targets, Proceedings of IEEE Aerospace Conference, Vol. 3 Big Sky, Montana, ISBN: 0-7803-5846-5, pp: 473 – 482, March, 2000
- Smith, D. and Singh, S. (2006). Approaches to Multisensor Data Fusion in Target Tracking: A Survey, IEEE Transactions on Knowledge and Data Engineering, Vol. 18, No. 12, (December 2006), pp. 1696 – 1710, ISSN: 1041-4347
- Steinberg A.; Bowman, C. & White, F. (1999). Revisions to the JDL Data Fusion Model, Proc. of the SPIE Sensor Fusion: Architectures, Algorithms, and Applications III, pp. 430-441, ISBN 0-8194-3193-1, Orlando, FL, USA, April 1999.
- Stubberud, A.R. (2000). “Constrained Estimate Of The State Of A Time-Variable System,” Proceedings of the 14th International Conference on Systems Engineering, Coventry, UK, pp. 513 – 518, September, 2000.
- Stubberud, A.R. (2003). “Sequential target tracking using constrained nonlinear estimators,” Proceedings of the 16th International Conference on Systems Engineering, Coventry, UK, ISBN 0-905949-91-9, pp. 652 – 656, September, 2003.
- Stubberud, S. and Kramer, K. (2006). Data Association for Multiple Sensor Types Using Fuzzy Logic, IEEE Transactions on Instrumentation and Measurement, Vol. 55, No. 6, (December 2006), pp: 2292 - 2303, ISSN: 0018-9456
- Stubberud, S. C., Kramer, K. (2007). Fuzzy Logic Based Data Association with Target/ Sensor Soft Constraints, Proceedings of the 2007 IEEE International Symposium on Intelligent Control, Singapore, ISBN: 978-1-4244-0441-4, pp. 620 – 625, October 2007
- Stubberud, S. and Kramer, K. (2009). Phase vs. Amplitude: Analysis of Optically-Based Correlation For Track Association, Proceedings of the IEEE International Conference of Systems Engineering. Coventry, UK, pp. 429-433, September 2009.
- Stubberud, S. and Kramer, K. (2010). Track-to-Track Association Using a Phase-Only Filter, Signal Processing, Sensor Fusion, and Target Recognition XIX - Proceedings of SPIE, Vol. 7697, Orlando, FL, ISBN: 9780819481610. pp. 733605.1-12, April 2010
- Stubberud, S. and Kramer, K. (2010). Incorporation of Measurement Uncertainty into Optically-Inspired Measurement-To-Track Data Association, Proceedings of the IEEE International Instrumentation and Measurement Technology Conference, San Antonio, TX, ISBN: 978-1-4244-2832-8. pp. 18-23, May 2010
- Stubberud, S. C., Kramer, K., Geremia, J. A. (2007). Feature Object Extraction: Evidence Accrual For The Level 1 Fusion Classification Problem. IEEE Transactions on Instrumentation and Measurement, Vol. 56, No. 6, (December 2007), pp. 2705-2716, ISSN: 0018-9456.
- Stubberud, S. and Lugo, K. (1999). A Fuzzy Logic Approach For Data Association, Sensor Fusion: Architectures, Algorithms, and Applications III, Proceedings of SPIE, vol. 3719, Orlando, FL, ISBN: 9780819431936, pp.242 – 249, April, 1999
- Stubberud, S.; Shea, P.J & Klamer, D. (2003). Data Fusion: A Conceptual Approach to Level 2 Fusion (Situational Awareness), Proceedings of SPIE, Aerosense03, pp. 455-462, ISBN 0-8194-4956-3, Orlando, FL., April 2003.
- Yang, C. and Blasch, E. (2009). Kalman Filtering With Nonlinear State Constraints, IEEE Transactions on Aerospace and Electronic Systems, Vol. 45, No. 1, (January 2009), pp. 70-84, ISSN 0018-9251



## **Sensor Fusion - Foundation and Applications**

Edited by Dr. Ciza Thomas

ISBN 978-953-307-446-7

Hard cover, 226 pages

**Publisher** InTech

**Published online** 24, June, 2011

**Published in print edition** June, 2011

Sensor Fusion - Foundation and Applications comprehensively covers the foundation and applications of sensor fusion. This book provides some novel ideas, theories, and solutions related to the research areas in the field of sensor fusion. The book explores some of the latest practices and research works in the area of sensor fusion. The book contains chapters with different methods of sensor fusion for different engineering as well as non-engineering applications. Advanced applications of sensor fusion in the areas of mobile robots, automatic vehicles, airborne threats, agriculture, medical field and intrusion detection are covered in this book. Sufficient evidences and analyses have been provided in the chapter to show the effectiveness of sensor fusion in various applications. This book would serve as an invaluable reference for professionals involved in various applications of sensor fusion.

### **How to reference**

In order to correctly reference this scholarly work, feel free to copy and paste the following:

Stephen C. Stubberud and Kathleen A. Kramer (2011). Data Association Techniques for Non-Gaussian Measurements, Sensor Fusion - Foundation and Applications, Dr. Ciza Thomas (Ed.), ISBN: 978-953-307-446-7, InTech, Available from: <http://www.intechopen.com/books/sensor-fusion-foundation-and-applications/data-association-techniques-for-non-gaussian-measurements>

**INTECH**  
open science | open minds

### **InTech Europe**

University Campus STeP Ri  
Slavka Krautzeka 83/A  
51000 Rijeka, Croatia  
Phone: +385 (51) 770 447  
Fax: +385 (51) 686 166  
[www.intechopen.com](http://www.intechopen.com)

### **InTech China**

Unit 405, Office Block, Hotel Equatorial Shanghai  
No.65, Yan An Road (West), Shanghai, 200040, China  
中国上海市延安西路65号上海国际贵都大饭店办公楼405单元  
Phone: +86-21-62489820  
Fax: +86-21-62489821

© 2011 The Author(s). Licensee IntechOpen. This chapter is distributed under the terms of the [Creative Commons Attribution-NonCommercial-ShareAlike-3.0 License](#), which permits use, distribution and reproduction for non-commercial purposes, provided the original is properly cited and derivative works building on this content are distributed under the same license.

IntechOpen

IntechOpen